Assessment of phase evolution in CaO–MgO–Al_2O_3–SiO_2 system with varied Al_2O_3/SiO_2 ratio using in-situ high-temperature Raman spectroscopy and X-ray scattering

F Gyakwaa[1], *S Wang* [2], *H Singh*[3], *G King*[4], *Q Shu*[5], *W Cao*[6], *M Huttula*[7], *T Fabritius*[8]

1. Postdoc, Process Metallurgy Research Unit, University of Oulu, FI-90014 Oulu, Finland. Email: Francis.Gyakwaa@oulu.fi.
2. Postdoc, Nano and Molecular Systems Research Unit, University of Oulu, FI-90014 Oulu, Finland. Email shubo.wang@oulu.fi.
3. Adjunct Professor, Nano and Molecular Systems Research Unit, University of Oulu, FI-90014 Oulu, Finland. Email: harishchandra.singh@oulu.fi.
4. Scientist, Canadian Light Source, 44 Innovation Blvd., Saskatoon, Saskatchewan S7N 2V3, Canada Email: Graham.King@lightsource.ca.
5. Professor, Process Metallurgy Research Unit, University of Oulu, FI-90014 Oulu, Finland Email: Qifeng.Shu@oulu.fi.
6. Professor, Nano and Molecular Systems Research Unit, University of Oulu, FI-90014 Oulu, Finland. Email: Wei.Cao@oulu.fi.
7. Professor, Nano and Molecular Systems Research Unit, University of Oulu, FI-90014 Oulu, Finland. Email: Marko.Huttula@oulu.fi.
8. Professor, Process Metallurgy Research Unit, University of Oulu, FI-90014 Oulu, Finland Email: timo.fabritius@oulu.fi.

Keywords: slag, *in-situ* synchrotron X-ray diffraction, Raman spectroscopy, crystallisation, structural properties.

ABSTRACT

Metallurgical slag, such as refining slag, is essential to enhance or promote steel cleanliness. The $CaO–MgO–Al_2O_3–SiO_2$ system is the primary source of oxides-based inclusions. It plays a vital role in applications in various pyrometallurgical processes. Numerous thermodynamic databases and physicochemical properties of slag studies mainly focus on quenched samples and measurements at room temperature. Consequently, the present study explored the physicochemical, structural properties, and crystallisation evolution for $CaO–MgO–Al_2O_3–SiO_2$ glassy slags via in situ high-temperature Raman spectroscopy and synchrotron X-ray diffraction. The study was carried out by synthesising $CaO–MgO–Al_2O_3–SiO_2$ slag with varying Al_2O_3/SiO_2 ratios. The results from the situ high-temperature measurement demonstrated a pattern showing a transformation of a broad peak from the glassy matrix to crystalline peaks. The study showed crystallisation of dominant phases such as Ca_2SiO_4, $Ca_2Al_2SiO_7$ and $CaAl_2O_4$ that correspond and are attributable to changes of structural units during in situ high-temperature measurements. The results further showed a correlation between an increase and transformation in crystalline phases observed from the spectra obtained from non-isothermal heating of the samples.

INTRODUCTION

Metallurgical slag, such as refining slag, is essential to enhance steel cleanliness (Lia & Dua, 2022; Sniegoň et al., 2021; Yoon et al., 2002; Yu et al., 2021). Promoting steel cleanliness includes optimising inclusion composition in ladle furnace refining, such as using the deoxidation process. Refining slag main components such as SiO_2, CaO, MgO, and Al_2O_3 can form the $CaO–MgO–Al_2O_3–SiO_2$ system. The $CaO–MgO–Al_2O_3–SiO_2$ system is the primary source of oxides-based inclusions predominantly for Al-deoxidized treated with calcium steels. This makes the optimisation of quaternary slag systems such as $CaO–MgO–Al_2O_3–SiO_2$ systems have an important role for secondary refining, such as for improving absorption of non-metallic inclusions and for refractory protection (Bielefeldt, Vilela & Heck, 2014; Jiang, Wang & Wang, 2012; Kim, H. et al., 2013; Ma et al., 2014; Xu et al., 2014; Xu, et al., 2015). Researchers have shown that the crystallisation behaviour of the $CaO–MgO–Al_2O_3–SiO_2$ slag system is essential in optimising its applications for various processes (Bielefeldt, Vilela & Heck 2013; Lin et al., 2023; Yao, Ma & Lyu, 2021). The work carried out by Jung & Sohn (2012) suggests this can be achieved by controlling the formation volume ratio of the crystalline phase to that of the amorphous phase in the slag. Also, detailed studies have been covered concerning thermodynamic and viscosities analysis of this slag system to enhance inclusions control and performance of mould fluxes mechanism (Gan, Xin & Zhou, 2017; Jiao et al., 2007; Shankar et al., 2007; Song, Shu & Sichen, 2011; Li et al., 2017; Lin et al., 2023). Considering the essential role of metallurgical slag constituting components such as SiO_2, CaO, MgO, and Al_2O_3, various detailed studies have aimed to examine the physicochemical and structural properties such as crystallisation behaviour (Pereira et al., 2023; Zhang et al., 2010).

To further explore $CaO–MgO–Al_2O_3–SiO_2$ quaternary slag for process optimisation, various studies have been conducted to examine the role of varying some components such as Al_2O_3/ SiO_2 ratios (Kim, H. et al., 2013; Liao et al., 2012; Wang & Sohn, 2018; Zhang et al., 2008). Various analytical techniques, such as hot thermocouple technique (Kashiwaya et al., 2007), confocal laser scanning microscopy (Wang & Sohn, 2018) and single hot thermocouple technique (Kashiwaya et al., 2007; Esfahani & Barati, 2018) to characterise this slag system. Raman spectroscopy has been demonstrated as a potential analytical technique for studying the constituents such as metallurgical slag for structural analysis, especially from recent studies under in situ high-temperature conditions (Wang et al., 2022; Zhang et al., 2023). However, to the present authors' knowledge, the in situ and high-temperature crystallisation transformation mechanism of $CaO–MgO–Al_2O_3–SiO_2$ slags with Al_2O_3/SiO_2 ratios is yet to be explored using Raman spectroscopy. Such a study will further contribute to understanding the role of SiO_2 as a network former and Al_2O_3 as a network intermediate for the crystallisation mechanism of $CaO–MgO–Al_2O_3–SiO_2$ based slags.

This work will explore the crystalline phase evolution of $CaO–MgO–Al_2O_3–SiO_2$ glassy slags with varying Al_2O_3/SiO_2 ratios using in situ high-temperature Raman spectroscopy. Raman spectroscopy will be used to analyse the network microstructure of the slag and the structural formation of the crystalline phase of the samples during the non-isothermal melt process. The in situ high-

temperature crystalline phases formation mechanism of CaO–MgO–Al_2O_3–SiO_2 glass slags with varying Al_2O_3/SiO_2 will also be investigated using high energy synchrotron X-ray diffraction (HE-SXRD). The glassy slag's transformation temperatures and crystallisation behaviours will be examined using a differential scanning calorimeter (DSC) thermogram. Furthermore, X-ray diffraction (XRD) analysis of in situ samples was also used to identify the final phases formed at room temperature. These analytical techniques provide comprehensive structural information about the glassy sample and its melt.

EXPERIMENTAL

Sample Preparation

Reagent-grade chemicals of aluminium oxide (α-Al_2O_3), calcium oxide (CaO), silicon dioxide (SiO_2), and magnesium oxide (MgO), a purity that ranged from 99.7% to 99.9% and supplied by Alfa Aesar were used to synthesise the experimental slag samples. A thorough moisture removal and mixing were carried out and pressed into pellets. The pellets were subsequently placed in a Pt crucible, sintered at a high temperature of 1450 °C in a chamber furnace and quenched to obtain the desired CaO–MgO–Al_2O_3–SiO_2 quaternary glassy slag. The elemental composition of the prepared samples was estimated using XRF, an Axios Max model from Panalytical. The XRF operates using SuperQ's analysis software with an X-ray generator Rh-tube. It has a maximum power of 4 kW. The glassy slag was also measured using X-ray diffraction (XRD) to determine how amorphous the samples prepared were, as shown in Figure 1. Details features concerning the XRD used for this work can be found in previous studies (Gyakwaa et al., 2019). The CaO–MgO–Al_2O_3–SiO_2 quaternary slag composition used for this study is shown in **Table 1**.

TABLE 1 – The experimental compositions (weight percentage, wt%) used to prepare the glassy slag samples and XRF analysis (wt%).

Pre-experimental composition									
Sample number	**Al_2O_3/ SiO_2**	**Chemical composition (wt%)**				**XRF (wt%)**			
		MgO	**Al_2O_3**	**SiO_2**	**CaO**	**MgO**	**Al_2O_3**	**SiO_2**	**CaO**
S1	0.30	5.00	15.00	50.00	30.00	5.62	14.45	50.2	29.73
S2	0.50	5.00	20.00	40.00	35.00	4.83	20.41	39.39	35.37
S3	0.83	5.00	25.00	30.00	40.00	5.61	24.73	29.88	39.78

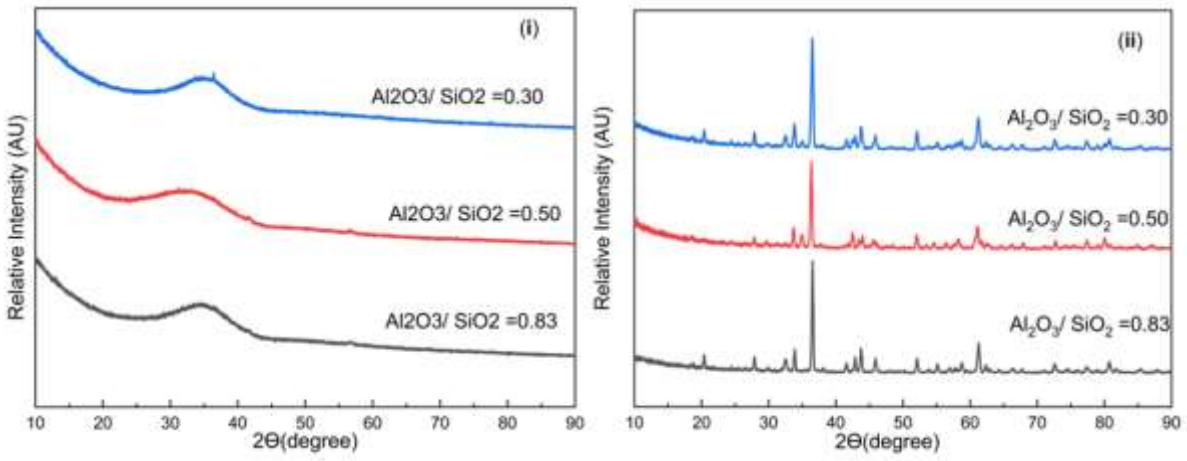

FIG 1 – XRD patterns of the (i) glassy slag samples and (ii) crystalline phase samples.

In-situ High-Temperature Raman Spectroscopic Measurements

The in-situ high-temperature Raman spectroscopy measurements of the glassy samples were performed using a reformative laser confocal micro-Raman spectrometer. The confocal micro-Raman spectrometer from B&W Tek (Plainsboro, US) utilises He-Cd laser with an excitation wavelength of 532 nm and is equipped with a rotatable stage. The in-situ Raman spectra from the sample were collected at room temperature and desired temperatures with a heating rate of 20 K/min, and a Raman spectral frequency range of 200 – 1200 cm^{-1} was used for this study. The desired temperatures selected for this study were room temperature, 760, 800, 850, 900, 1000, 1100, and 1200 °C. To achieve reproducibility for the acquired in situ Raman spectra, measurements were carried out by measuring the samples at least three times. The glassy samples were analysed using Raman spectroscopy at room temperature and subsequently in situ high temperature was carried to determine the melt structure and the influence of Al_2O_3/SiO_2 for sample matrix of CaO–MgO–Al_2O_3–SiO_2. The Raman Spectra obtained from the measurements were deconvolved using Gaussian line shapes (Mysen et al., 1982) for fitting the peaks that correspond to the vibrations of various structural units in the samples.

HE-SXRD and DSC Measurements

Experimental diffraction patterns were collected at every 100 °C from room temperature (RT) to 1000 °C, and then again one pattern after cooling to RT, following the heating. The data collection went well, with 30 keV photons for the proposed XRD measurements. A 2D Perkin Elmer area detector (200 × 200 μm^2 pixel size, 40 × 40 cm^2 in area) was placed behind the sample, allowing data acquisition in a Debye-Scherrer or transmission geometry. The refined wavelength was 0.4087 Å, and the sample to detector distance was 481.3 mm. Here, the exposure time was 0.5 s, and 120 snapshots were acquired to optimise the data collection and to ensure a reasonable statistic.

The crystallisation behaviours and transformation temperatures for glassy powder samples were determined by DSC measurements using a thermal analyser (model: STA 449 F3, Netzsch-Gerätebau Germany) with the purge gas as Ar. Temperature, balance, and sensitivity calibrations were performed prior to DSC measurements using metals with high purity and known melting points as reference materials. The platinum crucible without samples was used as reference material in obtaining the baseline. The glass powder samples were placed in the platinum crucible and heated to 1350 °C (a heating rate of 20 °C/min) to obtain the DSC signals and subsequently cooled to room temperature. The peak crystallisation temperatures, glass transition temperatures, and DSC continuous heating transformation (CHT) curves of crystalline phases from the measured samples were obtained from the DSC measurements.

RESULTS AND DISCUSSION

Raman Spectra Analysis

The relationship between the composition and structure of the prepared glassy slag samples is explored using Raman spectroscopy. The Raman spectra of the glassy CaO–MgO–Al_2O_3–SiO_2 quaternary samples obtained at room temperature with varying Al_2O_3/SiO_2 ratios of 0.30, 0.50 and 0.83 are presented in **Figure 2**. The Raman spectra could be divided into three frequency regions to contain dominant vibration bands. Between 420 – 600 cm^{-1} is a low-frequency region; between 600 – 800 cm^{-1} is a medium region, and the high-frequency region is between 850 – 1000 cm^{-1}. It can be observed from **Figure 2** that an increment in the Al_2O_3/SiO_2 ratio in the samples had a corresponding increase in the intensity of the Raman shift at a lower frequency region of 420 – 600 cm^{-1}. A corresponding decrease in the Raman shift in the region between 600 – 800 cm^{-1} was noticed when the ratio for Al_2O_3/SiO_2 increased for the samples.

Researchers have shown (Matson, Sharma & Philpotts, 1983; Han et al., 2016) that a Raman shift region between 420 – 600 cm^{-1} is associated with the activities of mixed stretching and bending vibration from the Al–O–Si bridge oxygen linkage, and a Raman frequency region between 600 – 800 cm^{-1} corresponds to mixed bending and stretching vibration occurring at of the Si–O–Si bridge oxygen linkage. Consequently, it can be estimated that the Al_2O_3/SiO_2 ratio influences the bridge oxygen linkage of Al–O–Si and Al–O–Si, where a rise in Al_2O_3/SiO_2 has a corresponding gradual

increase for the bridge oxygen linkage of Al–O–Si and a decrease for the bridge oxygen linkage of Si–O–Si.

The present study corresponds to the findings by (Mysen et al. 1982; Matson, Sharma & Philpotts, 1983; Han et al., 2016), suggesting that the existence of the Al–O–Si linkage is more possible compared to the combinations of Si–O–Si and Al–O–Al and attribution of the formation of the Al–O–Si linkage mostly in aluminosilicate glasses. With increasing Al_2O_3/SiO_2 ratios, it can also be noticed that within the higher frequency range 800 – 1100 cm^{-1}, the Raman peaks linked with the vibrations of depolymerised aluminosilicate and silicate units became more pronounced toward lower frequency. According to the studies conducted by Loewenstein (1954), which have a similar slag system as in this work, the tetrahedral $[AlO_4]^{5-}$ unit and tetrahedral $[SiO_4]^{4-}$ units structural can serve as the network formers.

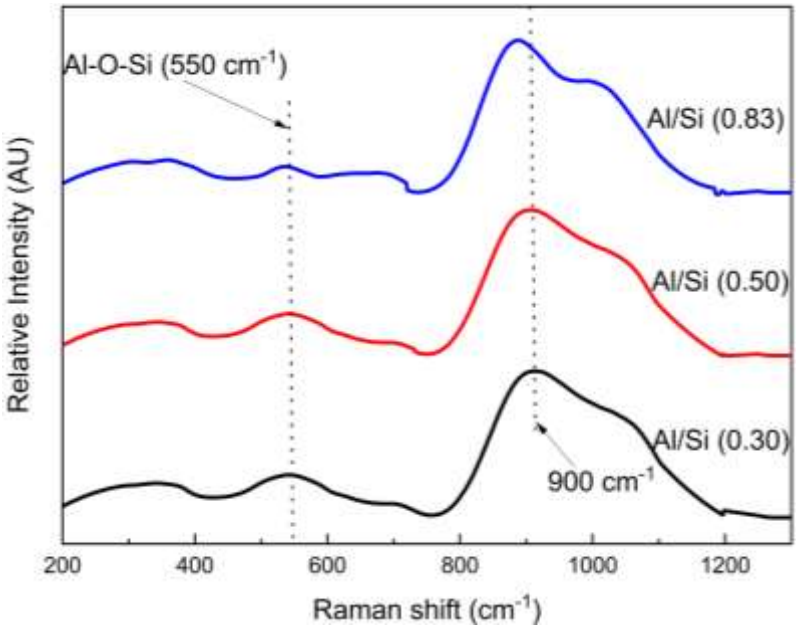

Fig 2 – Raman spectra for glassy samples with different Al_2O_3/SiO_2 ratios.

The Raman spectra obtained at room temperature were deconvoluted using the Gaussian-fitting method adopted by Mysen et al. (1982). It can be observed from the deconvoluted results obtained from the glassy samples before the in situ high temperature. Four main structural units of the symmetric stretching band of (SiO_4^{4-}) tetrahedra are represented as Q^n and n, denoted as a number of bridging oxygen in the tetrahedra for estimating the structural properties of the samples. Characteristic Raman bands at approximately 850 cm^{-1} are associated with silicate structure as monomer silicate units (Q^0) (Mysen et al., 1982) at approximately 900 for dimer silicate units (Q^1), at 950 cm^{-1} for chain-like silicate structures, Q^2 and 1030 cm^{-1} attributable to sheet-like silicate structures, Q^3, with corresponding BO/Al = 0, 1, 2, 3, as according to studies conducted by researchers (Li et al., 2014; Mysen et al., 1982; Wang et al., 2011) on silicate glasses. From the deconvolution results, the fitted Raman spectra full width at half maximum values were observed to reduce with a corresponding gradually raised Al_2O_3/SiO_2 ratio, which could be attributed to enhanced crystallisation ability compared with glass formation ability.

Figure 3 shows the Raman spectra for the slags with different Al_2O_3/SiO_2 ratios for estimating the sample's crystalline phases generated during heating and cooling. **Figure 3** is an illustrative example using sample 2 (Al_2O_3/SiO_2 = 0.50). In situ high-temperature Raman spectroscopy measurements were used to predict the crystalline phase formation from an amorphous phase in the slag system. It was noticed from the study that Raman spectra obtained from the glassy sample at room temperature did not significantly change until 500 °C. As the temperature increased from 500 °C, it was observed that the relative intensity of the Raman shift became sharper, indicating the formation of crystalline phases. It was evident when the sample was cooled to room temperature. Based on

the Raman shift positions, prominent crystalline phases such as Ca_2SiO_4, $CaAl_2O_4$ and $Ca_2Al_2SiO_7$ can be predicted when compared with reference Raman spectra (Allu et al., 2017; Bouhifd et al., 2002; Fujimori et al., 2002; Gyakwaa et al., 2019; Pešková, Machovič & Procházka, 2011; Remy, Reynard & Madon,1997).

Qualitative Raman spectra from in situ high-temperature measurements obtained from 700 – 1200 °C and cooling to room temperature show Raman bands (shifts) located at approximately 308, 440, 540, 600, 614, 634, 660, 724, 796, $cm^{-1,}$ which are characteristic of various phase attributable with this glassy samples (Allu et al., 2017; Bouhifd et al., 2002; Fujimori et al., 2002; Gyakwaa et al., 2019; Pešková, Machovič & Procházka, 2011; Remy, Reynard & Madon,1997). These Raman bands could be associated with the evolution of the glassy or amorphous phase and the formation of a crystalline phase since the crystallisation process is enhanced by increasing temperature. It was also observed that the Raman analysis from 600 °C to room temperature when cooling the samples during the in situ measurements showed no noticeable variation in the Raman spectra obtained, suggesting no significant crystalline phases were formed.

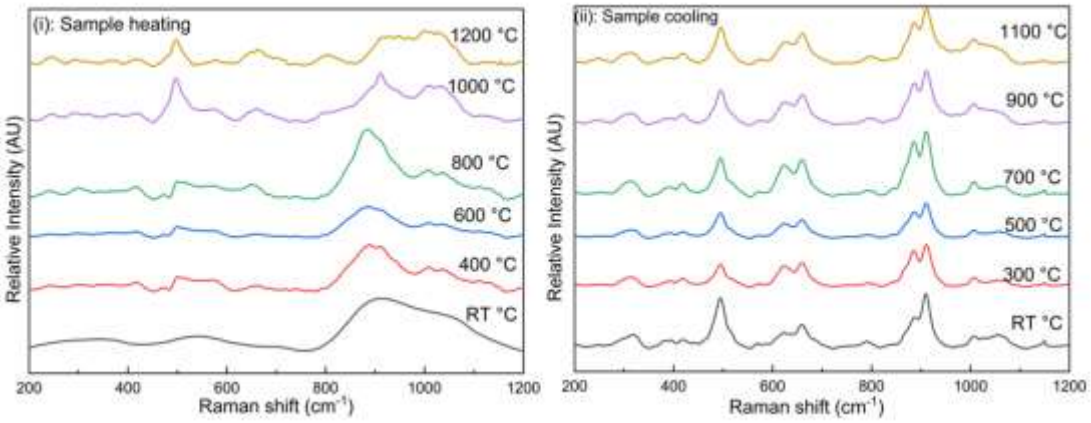

Fig 3 – Example to illustrate in situ high-temperature Raman spectra for the glassy samples (Al_2O_3/SiO_2 =0.50) during heat and cooling.

DSC and Identification of the crystalline phases using XRD

The thermogravimetric DSC curve of the glassy powder sample slag ($CaO–MgO–Al_2O_3–SiO_2$) with varied Al_2O_3/SiO_2 ratios using a heating rate of 20 °C/min is shown in **Figure 4**. It is observed from the DSC curve that the sample remained in a glassy state until approximately 600 °C. The exothermic peak noticed from the three samples had some variation corresponding to the Al_2O_3/SiO_2 mass percent ratio. The number of observed exothermic peaks gradually increases with a rise in the Al_2O_3/SiO_2 ratio. For instance, samples 2 and 3 increased with shoulder exothermic peaks appearing at 813 °C for sample 2 (A/S = 0.30); at 848 °C for sample 3 (A/S = 0.50), compared with sample 1(A/S = 0.30) at 801 °C. This feature can be attributable to the formation of more crystalline phases for samples 2 and 3. Therefore, it can be predicted that the crystallisation temperatures shift to higher temperatures with an increase in the Al_2O_3/SiO_2 ratio in the glassy samples. Sample 1's onset of crystallisation temperature is estimated at 780 °C, and samples 2 and 3 range from 750 – 780 °C. Therefore, the DSC analysis indicates that increasing the Al_2O_3/SiO_2 ratio tends to raise the crystallisation temperature and form more crystallisation ability Al_2O_3/SiO_2 ratios.

XRD was used to analyse the crystalline phases formed to identify further the various specific crystallisation products generated from the samples based on their varying Al_2O_3/SiO_2 ratios. In the in situ high-temperature Raman spectroscopy analysis, samples gradually cooled to room temperature, showing a predominantly mixture of crystalline phases from the study. These identified crystalline phases correspond and are consistent with qualitatively estimated phases based on their Raman band. Additionally, the samples obtained after DSC analysis were analysed using XRD, and crystalline phases formed during the cooling of the glassy slag were obtained. XRD analysis of the precipitated crystalline phases shows some variation in the slag analysis based on the characteristic

peaks of XRD. Crystalline phases of calcium silicate (Ca_2SiO_4) and calcium aluminosilicate ($Ca_2Al_2SiO_7$) showing for samples 1, 2 and 3 and additional crystalline phase of $CaAl_2O_4$ for sample 3. The additional phase of $CaAl_2O_4$ could be attributed to the transformation mechanism of Ca_2SiO_4 with increasing Al_2O_3 content in the CaO–MgO–Al_2O_3–SiO_2, as also previously shown by Yao, Ma & Lyu, (2021).

Subsequently, in situ high-temperature studies using high-energy synchrotron X-ray diffraction (HE-SXRD) were used to crystallise phases for the glassy samples. At room temperature, it can be easily observed that the diffraction pattern consists of a broad peak from the glassy matrix and three crystalline diffraction peaks. These crystalline peaks disappear until 700 °C, while new peaks show up. No significant change has been observed when heating onward to 900 °C. At 1000 °C, significant crystallisation is observed. A preliminary peak indexing from the HE-SXRD measurements suggests the crystalline phases heating to 1000 °C consist of mainly $Ca_2Al_2SiO_7$ and $CaAl_2O_4$ for the samples.

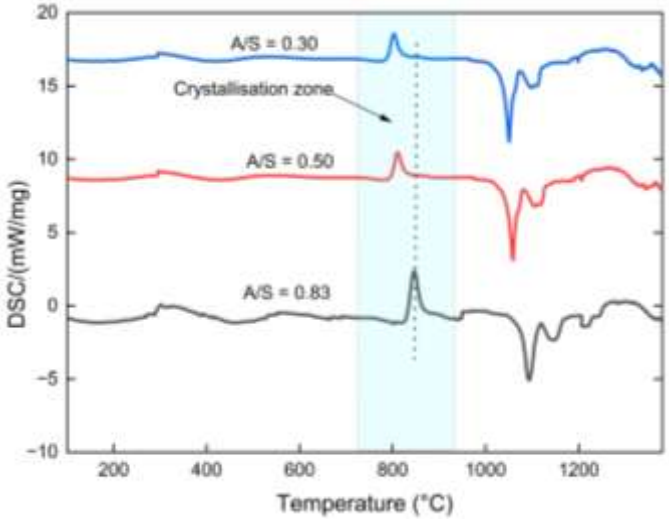

Fig 4. DSC curve of the glassy slag samples with different Al_2O_3/SiO_2 ratios analysis.

CONCLUSIONS

The present work examined the evolution of multicomponent crystalline phase products and the structural characterisation of glassy glassy Al_2O_3–CaO–SiO_2–MgO system. The effect with different Al_2O_3/SiO_2 ratios was explored by the DSC, XRF, XRD, in situ high-temperature Raman spectroscopy and high energy synchrotron X-ray diffraction (HE-SXRD) techniques. Based on the increase of the Al_2O_3/SiO_2 ratio in glassy slag. The findings from this study were concluded as follows:

- In-situ heating experiment using Raman spectroscopy and HE-SXRD, X-ray diffraction (XRD) analysis estimated primary crystalline phases of Ca_2SiO_4, $Ca_2Al_2SiO_7$ and with $CaAl_2O_4$ phases predicted at higher for Al_2O_3/SiO_2 ratio samples.
- Differential scanning calorimeter (DSC) thermogram crystallisation temperature increased with increasing Al_2O_3/SiO_2 ratio in the in situ heating experiment.
- The glassy slag shows types of bridge oxygen linkages and predicted the existence of a higher ratio of tetrahedral $[AlO4]^{5-}$ structural units with an increase in the $Al2O_3/SiO_2$ ratio where enhanced the polymerisation of tetrahedral $[SiO4]^{4-}$ and $[AlO4]^{5-}$ structural units improved from the Raman spectra analysis.

REFERENCES

Allu, A.R., Balaji, S., Tulyaganov, D.U., Mather, G.C., Margit, F. Pascual, M.J., Siegel, R. Milius, W. Senker, J. Agarkov, D.A., Kharton, V.V., Ferreira J.M.F., 2017. Understanding the Formation of $CaAl_2Si_2O_8$ in Melilite-Based Glass-Ceramics: Combined Diffraction and Spectroscopic Studies. ACS Omega. 2, 6233−6243.

Bielefeldt, W.V., Vilela, A.C.F., Heck N.C., 2014. Thermodynamic evaluation of the slag system CaO–MgO–SiO_2–Al_2O_3. AISTech. Iron Steel Technology Conference. Proc. 2, 1433–1445.

Bielefeldt, W.V., Vilela, C.A.F., Heck N.C., 2013. Evaluation of the slag system CaO-MgO-Al_2O_3-SiO_2. Technical contribution to the 44th Steelmaking Seminar, May, Araxá, MG, Brazil.

Bouhifd M.A., Gruener, G., Mysen, B.O., Richet, P., 2002. Premelting and calcium mobility in gehlenite ($Ca_2Al_2SiO_7$) and pseudowollastonite ($CaSiO_3$) Phys Chem Minerals 29: 655 – 662.

Esfahani, S., Barati, M., 2018. Effect of slag composition on the crystallisation kinetics of synthetic CaO-SiO_2-Al_2O_3-MgO slags, Metallurgical and Materials Transactions B 49 590–601.

Fujimori, H., Komatsu, H., Ioku, K., Goto S., 2002. Anharmonic lattice mode of Ca_2SiO_4: Ultraviolet laser Raman spectroscopy at high temperatures. Physical Review B 66, 064306.

Gan, L., Xin, J., Zhou, Y., 2017. Accurate viscosity calculation for melts in SiO_2–Al_2O_3–CaO–MgO systems. ISIJ International 57, 1303–1312.

Gyakwaa, F., Aula, M., Alatarvas, T., Vuolio, T., Huttula, M., Fabritius, T., 2019. Applicability of Time-Gated Raman Spectroscopy in the Characterisation of Calcium-Aluminate Inclusions. ISIJ International 59(10), 1846–1852.

Han, C., Chen, M., Rasch, R., Yu Y., Zhao B., 2016. Structure Studies of Silicate Glasses by Raman Spectroscopy. Advances in Molten Slags, Fluxes, and Salts: Proceedings of the 10th International Conference on Molten Slags, Fluxes and Salts 175–182.

Jiang, M., Wang, X.H., Wang, W. J., 2012. Study on refining slags targeting high cleanliness and lower melting temperature inclusions in Al killed steel. Ironmaking & Steelmaking 39, 20.

Jiao, K., Chang, Z., Chen, C., Zhang, J. L., 2007. Thermodynamic properties and viscosities of CaO–SiO_2–MgO–Al_2O_3 slags. Metall. Mater. Trans. B. 50, 1012–1022.

Jung, S.S., Sohn, I., 2012. Crystallisation behavior of the CaO-Al_2O_3-MgO system studied with a confocal laser scanning microscope. Metallurgical and Materials Transactions B 43 1530–1539.

Kashiwaya, Y., Nakauchi, T., Pham, K.S., Akiyama, S., Ishii, K., 2007. Crystallisation behaviors concerned with TTT and CCT diagrams of blast furnace slag using hot thermocouple technique, ISIJ International. 47 44–52.

Kim, H., Matsuura, H., Tsukihashi, F., Wang, W., Min D.J., Sohn I., 2013. Effect of Al_2O_3 and CaO/SiO_2 on the viscosity of calcium silicate-based slags containing 10 mass Pct MgO. Metallurgical and Materials Transactions B 44, 5–12.

Lia, S., Dua X., 2022. Effect of Al_2O_3 in Refining Slag on the Cleanliness and Fatigue Property of Ultra-low-carbon Automotive. Steel Materials Research.

Liao, J., Zhang, Y., Sridhar, S., Wang, X., Zhang, Z., 2012. Effect of Al_2O_3/SiO_2 ratio on the viscosity and structure of slags, ISIJ International 52, 753–758.

Lin, Y., Yi, Y., Fang, M., Ma, W., Liu W., 2023. Prediction Model for SiO_2 Activity in the CaO-Al_2O_3-SiO_2-MgO Quaternary Slag System. Minerals, 13, 509.

Li, J., Shu, Q., Chou, K., 2014. Structural study of glassy CaO-SiO_2-CaF_2-TiO_2 slags by Raman spectroscopy and MAS-NMR. ISIJ International 54, 721–727.

Li, S-j., Cheng, G-g., Yang, L., Chen, L., Yan, Q-z., Li C-w., 2017. A Thermodynamic Model to Design the Equilibrium Slag Compositions during Electroslag Remelting Process: Description and Verification 17), ISIJ International, 57, 4, 713–722.

Loewenstein, W., 1954. The distribution of aluminium in the tetrahedra of silicates and aluminates. Am. Mineral., 39, 92–97.

Matson, D.W., Sharma, S.K., Philpotts, J.A., 1983. The structure of high-silica alkali-silicate glasses. A Raman spectroscopic investigation. Journal of Non-Crystalline Solids. 58, 323–352.

Ma, W.J., Bao, Y.P., Wang, M., Zhao, D.W., 2014. Influence of slag composition on bearing steel cleanness. Ironmaking & Steelmaking 41(1), 26–30.

Mysen, B.O., Finger, L.W., Virgo, D., Seifert, F.A., 1982. Curve-fitting of Raman spectra of silicate glasses. American Mineralogist 67, 686–695.

Mysen, B., 2003. Physics and chemistry of silicate glasses and melts, in: Eur. J. Mineral. pp. 781–802.

Pešková, Š., Machovič, V., Procházka P., 2011. Raman spectroscopy structural study of fired concrete. Ceramics – Silikáty 55 (4) 410-417

Pereira, A., L., Pereira, J.A.M., Bielefeldt, W.V., Vilela A.C.F., 2023. Thermodynamic evaluation of viscosity behavior for $CaO–SiO_2–Al_2O_3–MgO$ slag systems examined at the temperatures range from 1500 to 1700 °C. Scientific reports Rep 13, 16274.

Remy, C., Reynard, B., Madon, M., 1997. Raman Spectroscopic Investigations of Dicalcium Silicate: Polymorphs and High-Temperature Phase Transformations. *Journal of the American Ceramic Society 80* (2), 413–423.

Shankar, A., Gornerup, M., Lahiri, A.K., Seetharaman, S., 2007. Experimental investigation of the viscosities in $CaO–SiO_2–MgO–Al_2O_3$ and $CaO–SiO_2–MgO–Al_2O_3–TiO_2$ slags. Metallurgical and Materials Transactions B 38, 911–915.

Sniegoň, M., Tkadlečková, T., Huczala, K, Michalek, Chudobová, L., Strouhalová, M., Walek, J., Pieprzyca, J., 2021. Thermodynamic analysis of $CaO - SiO_2 - Al_2O_3 - MgO$ slag system. Proceedings 30th Anniversary International Conference on Metallurgy and Materials 46-52

Song, M., Shu, Q., Sichen, D., 2011. Viscosities of the quaternary $Al_2O_3–CaO–MgO–SiO_2$ slags. Steel Research International 82, 260–268.

Wang, Z., Shu, Q., Chou, K., 2011. Structure of $CaO-B_2O_3-SiO_2-TiO_2$ Glasses: a Raman Spectral Study, ISIJ International.

Wang, Z., Sohn, I., 2018. Effect of the Al_2O_3/SiO_2 mass ratio on the crystallisation behavior of $CaO-SiO_2-MgO-Al_2O_3$ slags using confocal laser scanning microscopy, Ceramic International.

Wang, S., Rani, E., Gyakwaa, F., Singh, H., King, G., Shu, Q., Cao, W., Huttula, M., Fabritius, T., 2022. Unveiling Non-isothermal Crystallization of $CaO–Al_2O_3–B_2O_3–Na_2O–Li_2O–SiO_2$ Glass via In Situ X-ray Scattering and Raman Spectroscopy 61(18): 7017–7025.

Xu, J., Su, L., Chen, D., Zhang, J. & Chen, Y., 2015. Experimental investigation on the viscosity of $CaO–MgO(–Al_2O_3)–SiO_2$ slags and solid–liquid mixtures. Journal of Iron and Steel Research International 22(12), 1091–1097.

Xu, J.-F., Zeng, T., Sheng, M.-Q., Jie, C., Wan, K., Zhang, J.-Y., 2014. Viscosity of low silica $CaO–5MgO–Al_2O_3–SiO_2$ slags. Ironmaking and Steelmaking 41(7), 486–492.

Yao, Z., Ma, X., Lyu S., 2021. Phase equilibria of the $Al_2O_3–CaO–SiO_2$-(0%, 5%, 10%) MgO slag system for non-metallic inclusions control CALPHAD: Computer Coupling of Phase Diagrams and Thermochemistry 72 102227.

Yoon, B.-H., Heo, K.-H., Kim, J.-S., Sohn H.-S., 2002. Improvement of steel cleanliness by controlling slag composition Ironmaking and Steelmaking 29, 215.

Yu, H., Qiu, G., Zhang, J., X. Wang 2021. Effect of Medium Basicity Refining Slag on the Cleanliness of Al-killed Steel ISIJ International, 61 12, 2882–2888.

Zhang, Z., Wen, G., Tang, P., Sridhar, S., 2008. The influence of Al_2O_3/SiO_2 ratio on the viscosity of mold fluxes, ISIJ International 48 739–746.

Zhang, Z., Wen, G., Liao, J., Sridhar, S., 2010. Observations of crystallisation in mold slags with varying Al_2O_3/SiO_2 ratio, Steel Research International. 81 (2010) 516–528.

Zhang, B., Tekle, H., O'Malley, R. J., Sander, T., Smith, J. D., Gerald, R. E., Huang, J., 2023. In Situ and Real-Time Mold Flux Analysis using a High- Temperature Fiber-Optic Raman Sensor for Steel Manufacturing Applications Journal of Lightwave Technology. 41, 4419-4429.